

Synthesis, Characterisation, and Antimicrobial Activities of *S*-Benzyl- β -*N*-3-methoxybenzoyl Dithiocarbazate (SB3OME) and its Metal Complexes

Siti Khadijah Roslan and Fiona N. -F How*

Department of Chemistry, Kulliyah of Science, International Islamic University Malaysia (IIUM),
25200, Kuantan, Pahang, Malaysia

*Corresponding author (e-mail: howfiona@iium.edu.my)

A new substituted dithiocarbazate derivative ligand, *S*-benzyl- β -*N*-3-methoxybenzoyl dithiocarbazate (SB3OME) has been prepared *via* the nucleophilic substitution reaction of *S*-benzyl dithiocarbazate with *meta*-methoxybenzoyl chloride. A series of complexes of SB3OME with Cu(II), Zn(II), Co(II), and Ni(II) were also synthesised. These complexes have a general formula of $[M(SB3OME)_2]$, where M represents Cu^{2+} , Zn^{2+} , Co^{2+} , and Ni^{2+} . All the synthesised compounds were characterised using various physico-chemical techniques. It was found that all complexes exhibited a six-coordinate where SB3OME acts as a uninegatively charged tridentate NOS ligand, resulting in an octahedral geometry. The antimicrobial activities of all compounds against *Staphylococcus aureus* (ATCC 25923), *Bacillus cereus* (ATCC 11778), *Pseudomonas aeruginosa* (ATCC 27853), *Escherichia coli* (ATCC 25922) were evaluated. The values of minimum inhibitory concentration (MIC) were obtained in reference to gentamycin as the standard drug. MIC assay shows that $Cu(SB3OME)_2$ is the most active compound with a MIC value of 437 μ g/ml against *Staphylococcus aureus* (ATCC 25923) and *Pseudomonas aeruginosa* (ATCC 27853). This study concludes that the antimicrobial activities will enhance upon coordination with metal ions, and the metal complexes can be considered for further development as potential antibiotics.

Keywords: Dithiocarbazate derivatives; metal complexes; antimicrobial; minimum inhibitory concentration; tridentate

Received: January 2024; Accepted: August 2024

Antimicrobial drug resistance (AMR) is a global health threat that causes an increased risk of disease spread with the difficult-to-treat infections that have impacted the higher rates of illness, disability, and death linked to bacterial infections [1]. Current classes of antibiotics have limited efficacy against certain bacteria, such as *Mycobacterium tuberculosis* or *Pseudomonas aeruginosa*, which have developed resistance to multiple classes of antibiotics [1-2]. Therefore, there is an urgent demand for the discovery and supply of new antibacterial agents to effectively combat AMR. Metal-based compounds have emerged as potential candidates for treating microbial infections due to their distinct mode of action. Moreover, metal complexes offer various advantages over conventional antibiotics due to their broad-spectrum activity designed to target a range of bacterial species, making them potentially effective against a wide range of infections [3-4]. Plus, the metal complexes possess added advantages, which are extremely stable in different environmental situations, rendering them suitable for any circumstances, such as in the presence of bodily fluids or different pH conditions [5].

Metal complexes derived from dithiocarbazate derivatives received considerable interest due to their

promising bioactivities against a wide range of bacterial cells [6-7]. Dithiocarbazate derivatives contain thiosemicarbazide moiety (-NH-NH-C(=S)-) with a thiol group (-SH) attached to a central carbon atom (Figure 1). Interestingly, they have nitrogen and sulphur donor atoms, enabling them to form complexes with various metal ions. Metal complexes of dithiocarbazate derivatives have shown significant biological activities such as antibacterial properties [8-10] antifungal [11] antitumor [12] and anticancer [13-14].

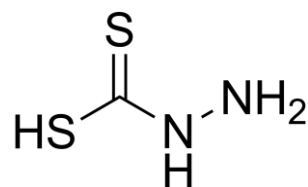


Figure 1. Dithiocarbazate backbone.

Therefore, we synthesised and characterised a new substituted dithiocarbazate derivative, *S*-benzyl- β -*N*-3-methoxybenzoyl dithiocarbazate (SB3OME), and its metal complexes. The antibacterial activities were determined using MIC assay against *Staphylococcus*

aureus (ATCC 25923), *Bacillus cereus* (ATCC 11778), *Pseudomonas aeruginosa* (ATCC 27853), and *Escherichia coli* (ATCC 25922).

EXPERIMENTAL

Chemicals and Materials

The solvent and chemicals used in this study were 3-methoxybenzoyl chloride, benzyl chloride, hydrazine hydrate, carbon disulfide, copper(II) acetate monohydrate, nickel(II) acetate tetrahydrate, zinc(II) acetate dihydrate, cobalt(II) acetate tetrahydrate, potassium hydroxide, absolute ethanol, silica gel, dimethyl sulfoxide, potassium bromide, nutrient agar, nutrient broth, gentamycin. All solvents and chemicals were used as received without purification and were purchased from Hmbg@ Chemicals, Acros Organics, Merck, Sigma Aldrich, R&M Chemicals, Bendosen, Fisher Scientific, Himedia, and VWR Life Science.

Instrumentation

Melting points were determined using Electrothermal™ IA9300. The IR spectra were recorded in the range of 400–4000 cm^{-1} using KBr pellets on a Perkin Elmer 96255 FT-IR spectrometer. The molar conductance of a 10^{-3} M solution of each metal complex in DMSO was measured using a Eutech CON 700 conductivity meter. The UV–VIS spectra were recorded on a Shimadzu UV-1900 Series PC spectrophotometer (800–200 nm) in DMSO solution. ^1H NMR and ^{13}C NMR spectra were recorded on NMR Bruker Ultra Shield Plus 500 MHz spectrometer using DMSO as the solvent. Thermogravimetric analysis was measured using the Thermogravimetric Analyzer Shimadzu TGA-50 Series. For TGA analysis, the nitrogen gas flow rate was 10 ml/min with a heating rate of 10 $^{\circ}\text{C}/\text{min}$. The starting temperature was 25 $^{\circ}\text{C}$, with the maximum temperature set at 500 $^{\circ}\text{C}$ and 800 $^{\circ}\text{C}$ for SB3OME and metal complexes, respectively. Magnetic susceptibility was measured with a Sherwood Scientific MSB AUTO at 298 K.

Preparation of *S*-benzylthiocarbazate (SBDTC)

SBDTC was synthesised as previously reported [15]. Potassium hydroxide (5.7g, 0.1 mol) dissolved in cold 90% ethanol (35.0 ml) was added with hydrazine hydrate (5.0 ml, 0.1 mol), and 5 ml of hydrazine hydrate (0.1 mol) was added to this solution. The mixture was placed in an ice-salt bath. Carbon disulphide (0.1 mol, 6 ml) was then added dropwise over an hour while continuously stirring with a mechanical stirrer. Upon completion, two layers formed, with the lower layer of brown oil being acquired and dissolved in 30 ml of cold, 40% ethanol. Benzyl chloride (0.1 mol, 11.37 ml) was added dropwise with the solution, which was maintained in an ice bath (0–5 $^{\circ}\text{C}$). After the benzyl chloride was fully added, a white precipitate was produced, filtered, and dried over silica gel overnight.

Preparation of *S*-benzyl- β -*N*-3-methoxybenzoyldithiocarbazate (SB3OME)

SB3OME was synthesised according to a reported study [16]. Potassium hydroxide (0.01 mol, 0.56 g) dissolved in absolute ethanol was added with SBDTC (0.01 mol, 1.983 g), which was dissolved in 30 ml of absolute ethanol. The solution was heated, and 3-methoxybenzoyl chloride (0.01 mol, 1.42 ml) was added dropwise while stirring and heating the solution continuously. The resultant solution was heated and stirred to reduce half its volume. The white precipitate was filtered and dried over silica gel. The product was recrystallised using methanol.

General Method for Preparation of Metal Complexes

Metal complexes were prepared based on the prior report [16]. A heated solution of metal salt (0.0009 mol) dissolved in absolute ethanol (30 ml) was added to SB3OME (0.0009 mol, 0.3 g) dissolved in the same solvent. For around 20 minutes, the mixture was heated and stirred continuously until half the volume. The precipitate was filtered while still hot and left to dry overnight on silica gel. The metal salts used were copper(II) acetate monohydrate (0.18 g), nickel(II) acetate tetrahydrate (0.22 g), zinc(II) acetate dihydrate (0.20 g), and cobalt(II) acetate tetrahydrate (0.22 g) are the metal salts that are used.

Bacteria Culture

Antimicrobial activity was done at the Microbiology Laboratory at the Physical Building, Kulliyah of Science, IIUM Kuantan Campus, International Islamic University Malaysia. Four pathogenic bacteria were cultivated in accordance with the reported literature [17]. All strains were kept at -80°C and streaked on nutrient agar plates, including *Staphylococcus aureus* (ATCC 25923), *Bacillus cereus* (ATCC 1778), *Escherichia coli* (ATCC 25922) and *Pseudomonas aeruginosa* (ATCC 27853). On nutrient broth, strains were cultivated at 37 $^{\circ}\text{C}$ for 24 hours prior to the antimicrobial assay. To prepare bacterial inocula, 3–4 colonies from the agar plate were selected and adjusted to the 0.5 McFarland standard solutions in nutrient broth. By measuring the optical density (OD) at 625 nm with a single-beam UV-Vis Spectrophotometer, the turbidity of the bacteria was identified. The ideal OD for bacteria is 0.1, which is also equivalent to 1.5×10^8 CFU/mL.

Antimicrobial Assay

The antimicrobial assay was done to determine the minimum inhibitory concentration (MIC, mg/mL), and the procedure was referred from past literature [18]. The concentrations of the synthesised compounds and positive control (gentamycin) were prepared in two-fold serial dilutions. Stock solution of the compounds was prepared as 7000 $\mu\text{g}/\text{ml}$ in DMSO. 100 μL of Nutrient broth stock was added to each well,

except for the first well. From that point onward, 200 μ L of synthesized compound or positive control was added into the first well of the plate, and serial dilutions were finished using a micropipette. 100 μ L of bacteria were added to all wells. The plates were incubated at 37°C for 24 hours. The lowest concentration of the compounds that showed no recognizable growth of microorganisms was considered the MIC value.

RESULTS AND DISCUSSION

Synthesis, Physical and Analytical Data

S-benzyl- β -*N*-3-methoxybenzoyl dithiocarbazate (SB3OME) is obtained from the reaction scheme shown in Figure 2. Starting from the precursor, SBDTC is obtained from nucleophilic substitution of benzyl chloride with dithiocarbazate [19]. The reaction likely proceeds through the attack of the dithiocarbazate on the electrophilic carbon of benzyl chloride, followed by the displacement of the chloride ion. SB3OME is also produced *via* nucleophilic substitution reaction of SBDTC with 3-methoxybenzoyl chloride in the presence of potassium hydroxide. SBDTC, being a weak base, can lose a proton

and become negatively charged due to resonance involving the nonbonding pair of electrons on the nitrogen atom [16]. This negative charge attacks the 3-methoxybenzoyl group, which then attaches to the β -nitrogen of SBDTC to form SB3OME. Lastly, SB3OME reacts with the metal ions in ethanol to form metal complexes, as shown in Figure 3. In the presence of metal ions, SB3OME behaves as a uninegatively charged ligand and coordinates to the transition metal ions through the deprotonation of nitrogen adjacent to thione sulfur, carbonyl oxygen, and thione sulfur donor atoms to form the respective metal complexes. The physical and analytical information of SBDTC, SB3OME, and its metal complexes are shown in Table 1. All analytical data obtained are in agreement with the proposed structures. All compounds' sharp melting points (around 1 to 3 °C) show that the compounds are pure. Generally, each compound produces a moderate to good yield, except for SB3OME, which produces only a 40% yield. The low yield of SB3OME is caused by 3-methoxybenzoyl chloride's incompatibility with a strong base, potassium hydroxide [20] resulting in undesired side reactions. The metal complexes displayed a darker color when compared to SBDTC and SB3OME.

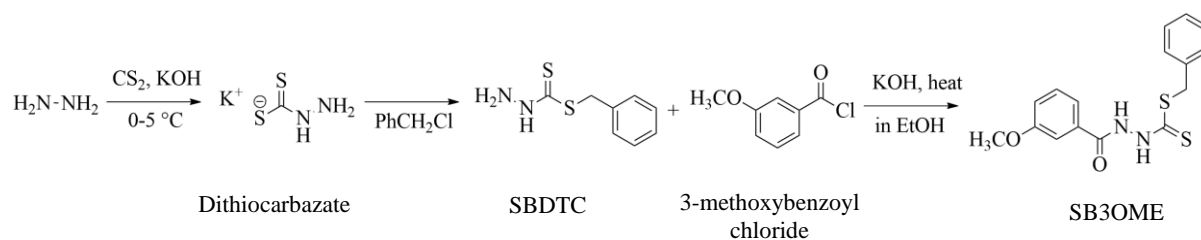


Figure 2. Synthesis scheme for the synthesis of SB3OME.

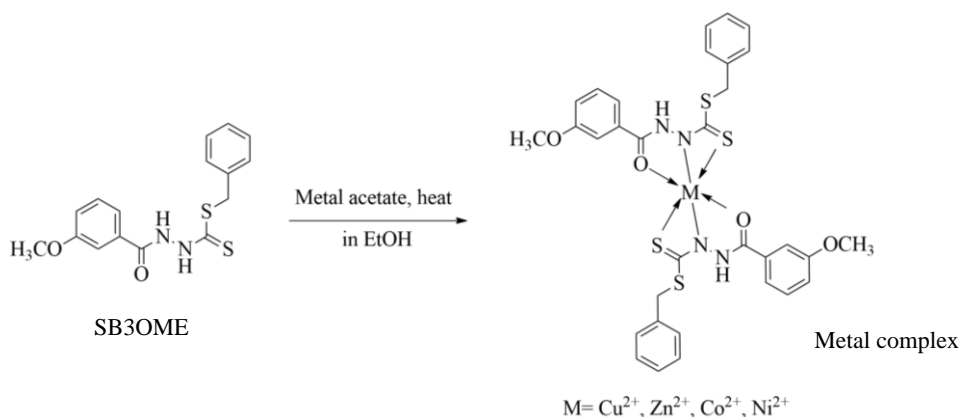
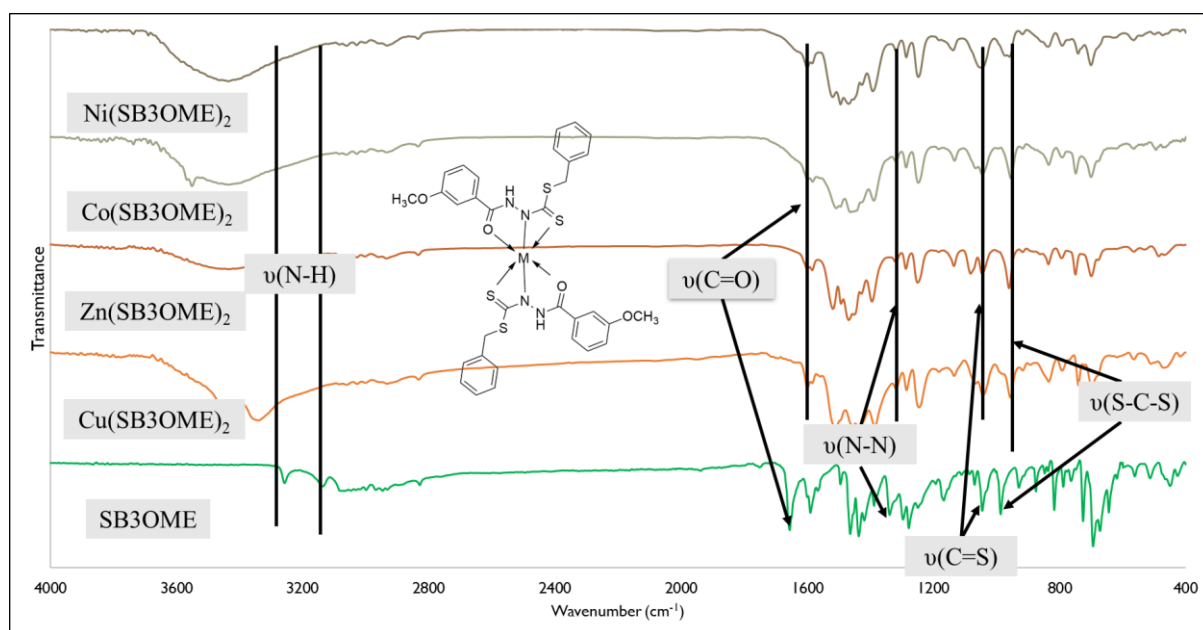
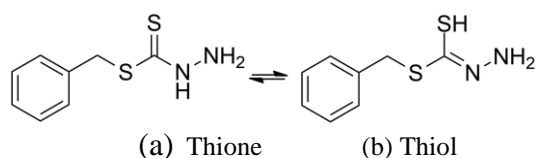


Figure 3. Reaction scheme of the formation of metal complexes from SB3OME.

Table 1. Physical data of SB3OME and its complexes.

| Compound | Colour | M.p (°C) | Found (Calculated %) | | | | Metal (%) | Yield (%) |
|-------------------------|--------|----------|----------------------|----------------|----------------|------------------|----------------|-----------|
| | | | C | H | N | S | | |
| SBDTC | White | 122-123 | - | - | - | - | - | 73 |
| SB3OME | White | 138-141 | 56.81 (57.81) | 4.30 (4.85) | 8.37 (8.43) | 19.54 (19.29) | - | 40 |
| Cu(SB3OME) ₂ | Black | 245-246 | 51.76 (52.76) | 4.22 (4.43) | 7.51 (7.69) | 17.03 (17.61) | 8.25 (8.72) | 61 |
| Zn(SB3OME) ₂ | White | 236-238 | 52.40 (52.63) | 4.70 (4.42) | 7.43 (7.67) | 17.39 (17.56) | 8.68 (8.96) | 65 |
| Co(SB3OME) ₂ | Green | 256-258 | 54.90 (53.10) | 4.35 (4.46) | 7.47 (7.74) | 18.87 (17.72) | - | 56 |
| Ni(SB3OME) ₂ | Brown | 226-228 | 51.30 (53.12) | 4.67 (4.46) | 7.68 (7.74) | 17.49 (17.72) | 8.29 (8.11) | 70 |

**Figure 4.** Overlay FTIR spectra of SB3OME and its metal complexes.**Figure 5.** Thione-thiol tautomerism of SBDTC.

Infrared Spectroscopy Spectra

The selected vibration bands of the synthesised compounds, as well as their assignments, are listed in

Table 2 and illustrated in Figure 4. Medium intensities bands are visible in the FTIR spectrum of SB3OME at 3258 and 3135 cm^{-1} , attributed to two $\nu(\text{N-H})$ groups attached to C=O and C=S groups, respectively.

SB3OME also shows peaks at 1658, 1340, 1047, and 986 cm^{-1} are assigned to $\nu(\text{C}=\text{O})$, $\nu(\text{N}-\text{N})$, $\nu(\text{C}=\text{S})$ and $\nu(\text{S}-\text{C}-\text{S})$ respectively. It is known that dithiocarbazate derivatives such as SBDTC can undergo thione-thiol tautomerism to become stable (Figure 5) [21]. However, SB3OME can undergo tautomerism, as shown in Figure 6 [16]. Thus, the presence of $\nu(\text{C}=\text{S})$ with $\nu(\text{C}=\text{O})$ and the disappearance of $\nu(\text{O}-\text{H})$ with $\nu(\text{S}-\text{H})$ in the FTIR spectra of SB3OME prove that these compounds exist as thione in solid form.

A comparison of the main vibrational bands of SB3OME is used to establish its ligating behavior in the metal complexes. Generally, despite the use of different metal ions to form SB3OME complexes, all FTIR spectra in this study exhibit a similar pattern, which is assumed to be in a similar coordination mode. One peak from $\nu(\text{N}-\text{H})$ disappeared about 3100 cm^{-1} , demonstrating that coordination happens through the proton of $\nu(\text{N}-\text{H})$ adjacent to thione sulfur. Consequently, $\nu(\text{N}-\text{N})$ at 1340 cm^{-1} also shifts to lower frequencies in all complexes near 1316-1318 cm^{-1} , proving that bonding occurs through hydrazinic nitrogen. The IR spectra of all metal complexes show a strong band at ~ 1600 cm^{-1} due to the $\nu(\text{C}=\text{O})$. The substantial negative shifts (-58 cm^{-1}) of $\nu(\text{C}=\text{O})$ indicate the involvement of carbonyl oxygen in bonding. Moreover, another negative shift of $\nu(\text{C}=\text{S})$ indicates that the metal ions coordinated with the thione sulphur, which is further supported by a significant negative shift (-32 cm^{-1}) of $\nu(\text{S}-\text{C}-\text{S})$. As a result, SB3OME exhibits an uninegative tridentate N, O, and S donor behaviour in the complexes by deprotonating upon complexation (Figure 3).

Nuclear Magnetic Resonance Spectra

From NMR spectra (Figure 7), it was found that SB3OME exists as thiol form, as depicted in Figure 6(b). The ^1H NMR spectrum displayed a singlet peak for H9 at $\delta_{\text{H}} = 10.53$ ppm corresponding to the N-H group. However, the integration value obtained was low (0.41) due to the proton exchange with water resulting to peak broadening and thus the reduced integration [22]. Furthermore, the appearance of another singlet peak at $\delta_{\text{H}} = 3.83$ ppm (H10), corresponding to S-H proton, further supports that SB3OME exists as the thiol form. Additionally, the methylene ($-\text{CH}_2$) proton was observed at $\delta_{\text{H}} = 4.51$ ppm (H11), while the methyl proton of the methoxy group ($\text{O}-\text{CH}_3$) was detected at $\delta_{\text{H}} = 3.81$ ppm (H8). Lastly, the aryl protons of the thiol SB3OME were found in the aromatic region at $\delta_{\text{H}} = 7.16-7.56$ ppm ($J=7-10$ Hz) (H1-H7). The ^{13}C NMR spectrum showed the thiol tautomeric form of SB3OME from the presence of $\text{C}=\text{N}$ at $\delta = 159.76$ ppm (C15) and the absence of $\text{C}=\text{S}$, which should occur at approximately $\delta = 200$ ppm. The carbonyl carbon, $\text{C}=\text{O}$ was found at $\delta = 166.03$ ppm (C14) is evident that SB3OME exists as the thiol tautomeric form and not the thiolol tautomeric form. A chemical shift at $\delta = 38.18$ ppm (C16) was assigned to the methylene ($-\text{CH}_2$) carbon, while the methoxy carbon, shielded by the aromatic ring, gave a chemical shift around $\delta = 55.81$ ppm (C13). The chemical shifts in the region of $\delta = 113 - 137$ ppm (C1-C12) were attributed to the aromatic carbons. Therefore, based on the result analyses of FTIR and NMR, SB3OME was found to exist as thione tautomeric form in solid state but as thiol tautomeric form in liquid state.

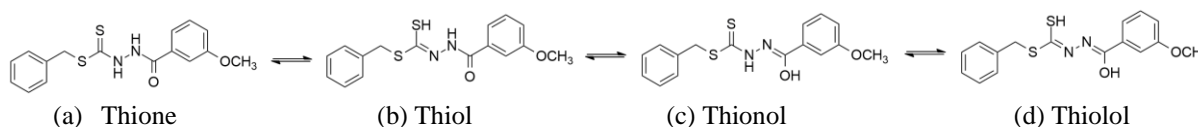


Figure 6. Thione-thiol-thionol-thiolol tautomerism of SB3OME.

Table 2. Selected IR bands of SBDTC, SB4OME and its metal complexes.

| Compound | IR bands (cm^{-1}) | | | | |
|------------------------------|-------------------------------|--------------------------|-----------------------------------|--------------------------|--------------------------|
| | $\nu(\text{N}-\text{H})$ | $\nu(\text{C}=\text{S})$ | $\nu(\text{S}-\text{C}-\text{S})$ | $\nu(\text{C}=\text{O})$ | $\nu(\text{N}-\text{N})$ |
| SBDTC | 3304, 3180 | 1048 | 952 | - | 1347 |
| SB3OME | 3258, 3135 | 1047 | 986 | 1658 | 1340 |
| $\text{Cu}(\text{SB3OME})_2$ | 3196 | 1041 | 954 | 1600 | 1316 |
| $\text{Zn}(\text{SB3OME})_2$ | 3194 | 1045 | 958 | 1601 | 1318 |
| $\text{Co}(\text{SB3OME})_2$ | 3192 | 1045 | 954 | 1600 | 1318 |
| $\text{Ni}(\text{SB3OME})_2$ | 3195 | 1040 | 955 | 1600 | 1318 |

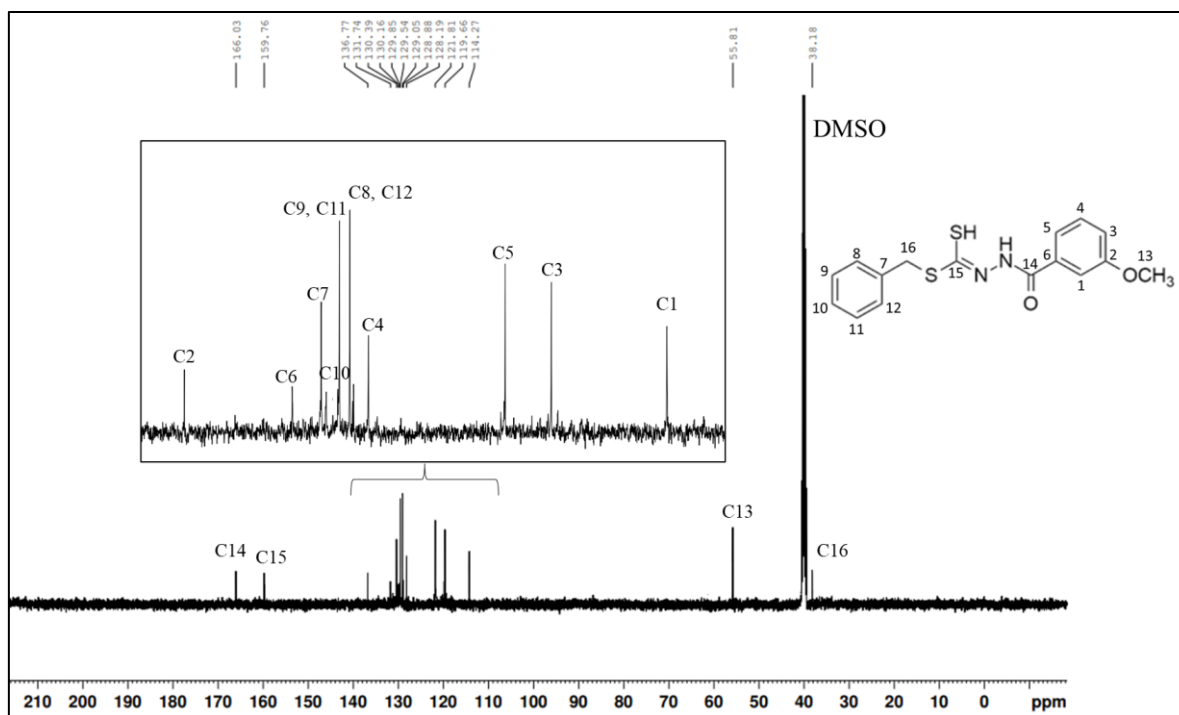
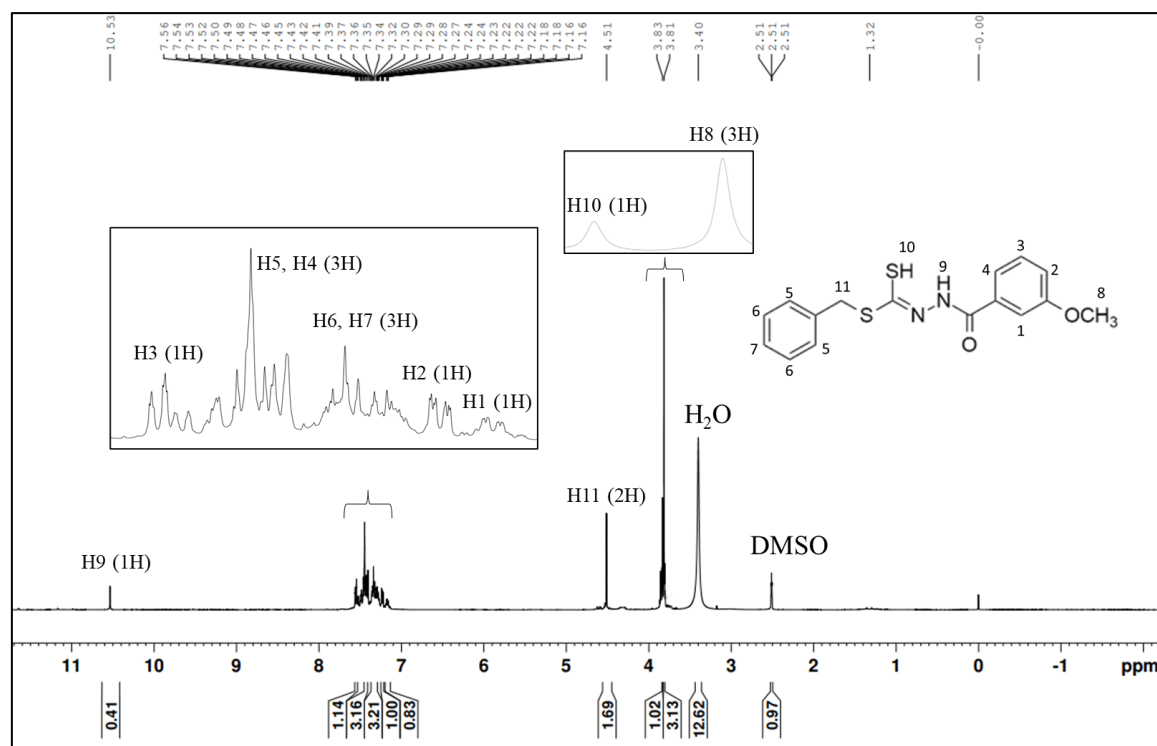


Figure 7. (a) ^1H -NMR and (b) ^{13}C -NMR spectra for SB3OME.

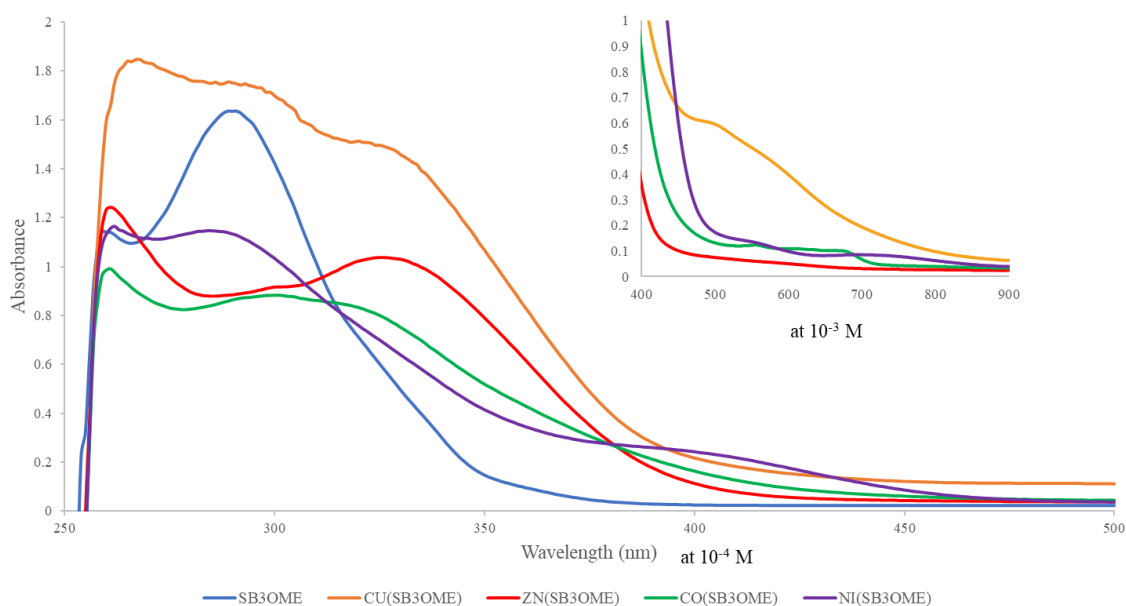


Figure 8. UV-Vis absorption spectra of SB3OME and its metal complexes.

Table 3. UV-Vis, molar conductivity data and magnetic moment data of SB3OME and its metal complexes.

| Compound | λ_{max} , nm (log ϵ , $cm^{-1} mol^{-1} L$) | Molar conductivity ($ohm^{-1} mol^{-1} cm^2$) | μ_{eff} (B.M.) |
|-------------------------|---|---|--------------------|
| SB3OME | 260 (4.056), 293 (4.214) | - | - |
| Cu(SB3OME) ₂ | 269 (4.266), 297 (4.238), 329 (4.17), 506 (2.767) | 2.81 | 1.897 |
| Zn(SB3OME) ₂ | 261 (4.091), 330 (3.946) | 2.45 | Diamagnetic |
| Co(SB3OME) ₂ | 258 (4.014), 318 (3.945), 674 (1.944) | 8.37 | 4.944 |
| Ni(SB3OME) ₂ | 264 (4.061), 289 (4.059), 407 (3.359), 563 (2.107), 750 (1.903) | 21.5 | 2.270 |

Conductivity Data

Conductivity data is tabulated in Table 3. All the metal complexes display molar conductivities between 2.4 to 21.5 $ohm^{-1} mol^{-1} cm^2$, showing that they are non-electrolyte in DMSO due to conductivity values being less than 50 $ohm^{-1} mol^{-1} cm^2$ [23]. Consequently, none of the complexes dissociate in solution, suggesting that SB3OME are [24].

Magnetic Moment

The electronic absorption spectral bands and the magnetic moments are listed in Table 3. Cu(SB3OME)₂ shows magnetic moments of 1.897 B.M, indicating one unpaired electron. Hence, it is expected to have octahedral geometry around the copper(II) ion [25]. As expected, Zn(SB3OME)₂ shows diamagnetic properties due to the d^{10} electron configuration [26]. The diamagnetic Zn(II) complex is expected to be six-coordinated and to have an octahedral structure. Based on the magnetic moment of the cobalt(II) complex (4.944 B.M), it is expected that the cobalt(II) ion is surrounded in an octahedral geometry in Co(SB3OME)₂ [27]. Lastly, paramagnetic Ni(SB3OME)₂ shows a magnetic moment

value of 2.270 BM, indicating two unpaired electron configurations suggesting octahedral geometry [28].

Electronic Spectra

In Table 3, the electronic spectrum data of SB3OME and its metal complexes are shown. According to Guo et al. (2006), the SB3OME's spectrum exhibits high-intensity bands at 260 and 293 nm, which are associated with the benzene rings' $\pi \rightarrow \pi^*$ and $n \rightarrow \pi^*$ transitions, respectively [29]. The metal complexes show a bathochromic shift around 288-300 nm, which can only occur upon complexation with metal ions due to the electronegativity properties of the metal ions [30]. Additionally, a band between 318 and 407 nm are identified as the ligand-to-metal charge transfer (LMCT) transition [25]. Furthermore, only the Zn(II) complex is found to be absent of the low-intensity band at 500-800 nm (Figure 8) due to the forbidden $d \rightarrow d$ transition [6]. According to Ramesh et al. (2016), the copper(II) complex exhibits low-energy $d \rightarrow d$ transitions at 506 nm, designated to the transition ${}^2E_g \rightarrow {}^2T_{2g}$ that suggests the copper complex adopted an octahedral geometry [31]. The octahedral cobalt(II) complex displays a broad peak at 674 nm, indicating

the transition ${}^4T_{1g}(F) \rightarrow {}^4T_{2g}(F)$ [32]. The appearance of a low-intensity peak at 563 and 750 nm, which corresponds to the transitions of ${}^3A_{2g} \rightarrow {}^3T_{1g}(F)$ and ${}^3A_{2g} \rightarrow {}^3T_{2g}(F)$, respectively, in the nickel(II) complex, shows that the complex has an octahedral geometry. Overall, all the complexes are suggested to adapt to an octahedral geometry, as evidenced by the result of the electronic spectra.

Thermogravimetric Analysis

Thermal stability and decomposition data of all compounds are listed in Table 4. Generally, the TGA curve of SB3OME and metal complexes show two and three thermal decomposition stages, respectively (Figure 9). SB3OME is thermally stable in the temperature range 0-165 °C. Decomposition of the SB3OME initiates at 166 °C and finishes at 351 °C with two stages. In the first stage, there is a mass loss of 14.58% (Calc. 19.28%) at a temperature range of 166-230 °C due to the loss of the benzyl group from dithiocarbazate [33]. The other parts of SB3OME decompose in the second subsequent stage, with a loss of 70.90% (Calc. 63.54%) at 230 to 351 °C and gradually decreases till 500 °C. The remaining residue may be due to some trace amount of elemental sulfur, which does not decompose till 500 °C with a percentage mass of 14.51% (Calc. 13.26%) [33].

All the complexes displayed thermal decomposition through three stages. For $\text{Cu}(\text{SB3OME})_2$, the benzyl group from dithiocarbazate is decomposed at 162-243 °C with a loss of 24.56% (Calc. 25.09%). Then, it is followed by the decomposition of the methoxybenzoyl unit with a percentage mass of 28.70 (Calc. 29.49%) at around 243 to 363 °C. Lastly, CS_2 , with a mass of 21.19% (Calc. 20.96%), is removed

at a higher temperature of 363-700 °C. The residue left at about 25.55% (Calc. 24.45%) might be from CuO_2 and CuN [34]. Similar patterns are observed in the decomposition stage of $\text{Zn}(\text{SB3OME})_2$ and $\text{Ni}(\text{SB3OME})_2$. The benzyl group from the dithiocarbazate structure decomposed around 211-350 °C, with a mass of 33.44% (Calc. 33.83%) and 32.43 (Calc. 34.10%), respectively. The SCN group, which has a mass of 15.28% (Calc. 15.9%) and 17.43% (Calc. 16.09%), respectively, then loses around 320-450 °C. The other significant loss of 25.74% (Calc. 29.42%) and 23.82% (Calc. 29.69%), respectively, are assigned for the loss of methoxybenzoyl group at around 450 to 800 °C with the insignificant loss after 600 °C. The final products of $\text{Zn}(\text{SB3OME})_2$ and $\text{Ni}(\text{SB3OME})_2$ are of either metal oxide or metal nitride with a mass of 25.54% (Calc. 20.80%) and 26.321% (Calc. 20.06%), respectively.

On the other hand, unlike the other metal complexes, $\text{Co}(\text{SB3OME})_2$ exhibits the least final product with only 10.05% (Calc. 12.6%) of mass residue, which is expected due to the remaining cobalt oxide. Moreover, the pattern of the decomposing stage is different from other metal complexes in which the methoxybenzoyl group starts to decompose around 175 to 300 °C with a loss of 38.71% (Calc. 37.21%), followed by the SCN group is removed at 300-440 °C with a mass of 15.89% (Calc. 16.09%). The last stage encompasses the removal of benzyl unit from dithiocarbazate with a loss of 35.35% (Calc. 34.12%) at 440 to 800 °C. Thus, from the thermal stability analysis, every compound shows a different pattern of decomposing stage against the temperature. Furthermore, TGA analysis also shows that the complexes are more thermally stable than SB3OME upon complexation due to the presence of metal ions.

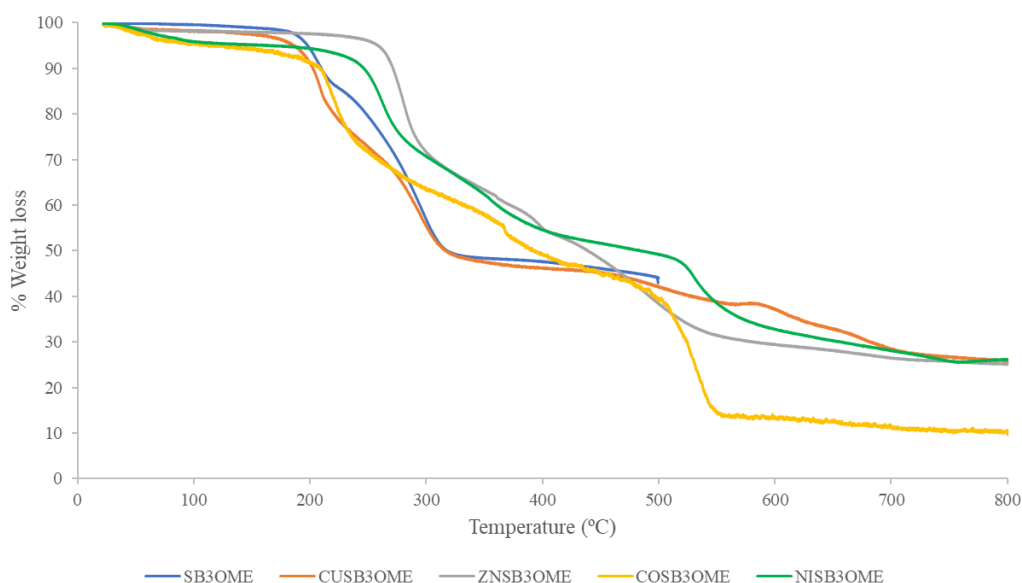


Figure 9. TGA curve of SB3OME and its metal complexes.

Table 4. Thermal properties of SB3OME and its metal complexes.

| Compound | Total weight loss (%) | Decompose temperature (°C) | DTG temperature (°C) | Percentage loss (%) |
|-------------------------|-----------------------|----------------------------|----------------------|---------------------|
| SB3OME | 85.485 | 166-230 | 205.09 | 14.58 |
| | | 230-500 | 283.37 | 70.90 |
| Cu(SB3OME) ₂ | 74.453 | 162-243 | 207.6 | 24.56 |
| | | 243-363 | 299.03 | 28.70 |
| | | 363-800 | 612.01 | 21.19 |
| Zn(SB3OME) ₂ | 74.458 | 226-350 | 284.07 | 33.44 |
| | | 350-420 | 393.45 | 15.28 |
| | | 420-800 | 493.64 | 25.74 |
| Co(SB3OME) ₂ | 89.950 | 175-300 | 215.48 | 38.71 |
| | | 300-440 | 373.66 | 15.89 |
| | | 440-800 | 538.32 | 35.35 |
| Ni(SB3OME) ₂ | 73.679 | 211-320 | 263.25 | 32.43 |
| | | 320-450 | 355.91 | 17.43 |
| | | 450-800 | 532.46 | 23.82 |

Antimicrobial Assay

Table 5 displays the minimum inhibitory concentration of all synthesised compounds in this study against gram-positive and gram-negative bacteria. The MIC values of SB3OME against these bacteria are between 437-875 $\mu\text{g/ml}$. Moreover, metal complexes of SB3OME also have MIC values in a similar range between 437 to 1750 $\mu\text{g/ml}$. These values indicate that SB3OME and its metal complexes are not as effective as gentamycin (MIC= <109 $\mu\text{g/ml}$). The inhibitory activity of all the complexes against *Staphylococcus aureus* (ATCC 25923) is better and requires only half the concentration compared to the precursors. The chelation is likely the main cause of the observed activity in the metal complexes. Upon complexation with the metal ions, the complexes become more liposoluble. As a result, it facilitates penetration of the cell membrane's lipid layer. Furthermore, a variety of parameters, including the chelate effect, should be considered for the antibacterial activities of the metal complex, including the nature of the ligands, the total charge of the complex, and the nature of the ion that neutralizes the given ionic complex [35], [36]. Contrarily, against *Bacillus cereus* (ATCC 11778), all metal complexes are less active than SB3OME, with the exception of Cu(SB3OME)₂, which shows similar inhibitory activity (MIC=875 $\mu\text{g/ml}$). SB3OME and its metal complexes, on the other hand, have a similar

toxicity level against *Escherichia coli* (ATCC 25922), with a MIC of 875 $\mu\text{g/ml}$. However, SB3OME is more effective than SBDTC against *Pseudomonas aeruginosa* (ATCC 27853), followed by both of its complexes, Cu(SB3OME)₂ and Zn(SB3OME)₂.

To analyse and explain the biological activity of all synthesised compounds, it is crucial to consider the contribution of the metallic ion, the ligand and the metal complex as an independent molecule, or the synergistic effects of two or three of these components. Generally, when comparing all potency of synthesised compounds, the most potent combination against these bacteria is Cu(SB3OME)₂, followed by SB3OME and Zn(SB3OME)₂, whilst Co(SB3OME)₂ and Ni(SB3OME)₂ are of similar level of potency. Thus, this activity is believed to be caused by several factors, including the ability of the metal complexes to disrupt bacterial cell membranes, inhibit enzymes involved in bacterial metabolism, and generate reactive oxygen species that can damage bacterial DNA. For instance, it has been noted that copper ions are efficient against fungi and bacteria and that their activity would rise in a complex [37], [38]. Plus, copper-based compounds have been shown to have antibacterial activity against antibiotic-resistant strains of bacteria, such as *Escherichia coli* [39], [40], [41]. Therefore, these characteristics make them excellent candidates for future antibacterial agents.

Table 5. Antimicrobial activity of SB3OME ligand and its metal complexes.

| Compound | MIC (ug/ml) | | | |
|-------------------------|---|-------------------------------------|--------------------------------------|--|
| | Gram-positive bacteria | | Gram-negative bacteria | |
| | <i>Staphylococcus aureus</i> (ATCC 25923) | <i>Bacillus cereus</i> (ATCC 11778) | <i>Escherichia coli</i> (ATCC 25922) | <i>Pseudomonas aeruginosa</i> (ATCC 27853) |
| SBDTC | 875 | 437 | 437 | 875 |
| SB3OME | 875 | 875 | 875 | 437 |
| Cu(SB3OME) ₂ | 437 | 875 | 875 | 437 |
| Zn(SB3OME) ₂ | 437 | 1750 | 875 | 437 |
| Co(SB3OME) ₂ | 437 | 1750 | 875 | 875 |
| Ni(SB3OME) ₂ | 437 | 1750 | 875 | 875 |
| Gentamycin | <109 | <109 | <109 | <109 |

CONCLUSION

In this work, SB3OME and its respective Cu(II), Zn(II), Co(II) and Ni(II) complexes were successfully synthesised and characterised. IR spectrum shows that SB3OME coordinates *via* deprotonation of the amino group, carbonyl oxygen, and thione sulfur to form metal complexes. The FTIR and NMR results of SB3OME reveal that SB3OME exists as thione in solid but as thiol tautomer in the liquid state. All metal complexes exhibit a neutral state based on their low conductivity values. From the UV-Vis absorption and magnetic susceptibility result, it can be determined that all metal complexes are of octahedral geometry. Thermogravimetric analyses display that the metal complexes exhibit greater thermal stability compared to SB3OME. The antimicrobial assay depicts Cu(SB3OME)₂ as the most effective compound against *Staphylococcus aureus* and *Pseudomonas aeruginosa* with a minimum inhibitory concentration of 437 μ g/ml. Thus, in this study, it is proven that the antimicrobial activity of the ligand is enhanced upon complexation due to an increase in lipophilicity during chelation.

ACKNOWLEDGMENTS

The authors thank the Department of Chemistry, Kulliyah of Science, International Islamic University Malaysia Kuantan, for the provision of laboratory facilities. An appreciation was also given to Associate Professor Dr. Nadiyah Halim from Universiti Malaya for her assistance in magnetic susceptibility analysis.

The authors declare that they have no conflict of interest.

REFERENCES

- Centers for Disease Control, U. (2019) *Antibiotic Resistance Threats in the United States, 2019*.
- Hameed, H. M. A., Islam, M. M., Chhotaray, C., Wang, C., Liu, Y., Tan, Y., Li, X., Tan, S., Delorme, V., Yew, W. W., Liu, J. & Zhang, T.

(2018) Molecular targets related drug resistance mechanisms in MDR-, XDR-, and TDR-Myco-bacterium tuberculosis strains. *Frontiers in Cellular and Infection Microbiology*, **8**.

- Pandey, A., Savino, C., Ahn, S. H., Yang, Z., Van Lanen, S. G. & Boros, E. (2019) Theranostic gallium siderophore ciprofloxacin conjugate with broad spectrum antibiotic potency. *Journal of Medicinal Chemistry*, **62(21)**, 9947–9960.
- Simpson, P. V., Desai, N. M., Casari, I., Massi, M. & Falasca, M. (2019) Metal-based antitumor compounds: beyond cisplatin. *Future Medicinal Chemistry*, **11(2)**, 119–135.
- Cuprys, A., Pulicharla, R., Brar, S. K., Drogui, P., Verma, M., & Surampalli, R. Y. (2018). Fluoroquinolones metal complexation and its environmental impacts. *Coordination Chemistry Reviews*, **376**, 46–61.
- Bhat, R. A., Singh, K., Kumar, D., Kumar, A. & Mishra, P. (2022) Antimicrobial studies of the Zn(II) complex of S-benzyl- β -(N-2-methyl-3-phenylallylidene) dithiocarbazate, **75(7–8)**, 1050–1062.
- Sohtun, W. P., Kathiravan, A., Asha Jhonsi, M., Aashique, M., Bera, S. & Velusamy, M. (2022) Synthesis, crystal structure, BSA binding and antibacterial studies of Ni (II) complexes derived from dithiocarbazate based ligands. *Inorganica Chimica Acta*, **536**, 120888.
- Adly, O. M. I. & El-Shafiy, H. F. (2019) New metal complexes derived from S-benzyl dithiocarbazate (SBDTC) and chromone-3-carboxaldehyde: synthesis, characterization, antimicrobial, anti-tumor activity and DFT calculations. **72(2)**, 218–238.
- Azam, M., Bitu, M. N. A., Mohapatra, R. K., Al-Resayes, S. I., Pintilie, L., Wabaidur, S. M., Al-

- qahtani, F. F., Islam, M. S., Sarangi, A. K. & Kudrat-E-Zahan, M. (2021) Synthesis, characterization of Uranyl (VI), Th (IV), Zr (IV) mixed-ligand complexes with *S*-methyl-2-(4-methoxybenzylidene) dithiocarbazate and N-donor co-ligand, and their evaluation as antimicrobial agent. *Journal of Saudi Chemical Society*, **25**(3).
10. Latif, M. A., Tofaz, T., Chaki, B. M., Tariqul Islam, H. M., Hossain, M. S. & Kudrat-E-Zahan, M. (2019) Synthesis, characterization, and biological activity of the Schiff base and its Ni(II), Cu(II), and Zn(II) complexes derived from 4-(dimethyl-amino) benzaldehyde and *S*-benzylidithiocarbazate. *Russian Journal of General Chemistry*, **89**(6), 1197–1201.
 11. Mohapatra, R. K., Sarangi, A. K., Azam, M., El-ajaily, M. M., Kudrat-E-Zahan, M., Patjoshi, S. B. & Dash, D. C. (2019) Synthesis, structural investigations, DFT, molecular docking and antifungal studies of transition metal complexes with benzothiazole based Schiff base ligands. *Journal of Molecular Structure*, **1179**, 65–75.
 12. Ramilo-Gomes, F., Addis, Y., Tekamo, I., Cavaco, I., Campos, D. L., Pavan, F. R., Gomes, C. S. B., Brito, V., Santos, A. O., Domingues, F., Luís, Â., Marques, M. M., Pessoa, J. C., Ferreira, S., Silvestre, S. & Correia, I. (2021) Antimicrobial and antitumor activity of *S*-methyl dithiocarbazate Schiff base zinc (II) complexes. *Journal of Inorganic Biochemistry*, **216**.
 13. How, F., Ibrahim, Z. & Zulkifli, N. I. (2018) Molecular docking of substituted Schiff bases derived from *S*-benzylidithiocarbazate as potential anticancer agents. *Frontiers in Pharmacology*, **9**.
 14. Md Yusof, E. N., Latif, M. A. M., Tahir, M. I. M., Sakoff, J. A., Veerakumarasivam, A., Page, A. J., Tiekink, E. R. T. & Ravoof, T. B. S. A. (2020) Homoleptic tin(IV) compounds containing tridentate ONS dithiocarbazate Schiff bases: Synthesis, X-ray crystallography, DFT and cytotoxicity studies. *Journal of Molecular Structure*, **1205**, 127635.
 15. Ali, M. A. & Bose, R. (1977) Metal complexes of Schiff bases formed by condensation of 2-methoxybenzaldehyde and 2-hydroxybenzaldehyde with *s*-benzylidithiocarbazate. In *J. Inorg Nucl. Chem.*, **39**.
 16. How, F. N. F., Crouse, K. A., Tahir, M. I. M., Tarafder, M. T. H. & Cowley, A. R. (2008) Synthesis, characterization and biological studies of *S*-benzyl- β -*N*-(benzoyl) dithiocarbazate and its metal complexes. *Polyhedron*, **27**(15), 3325–3329.
 17. Malmberg, C., Yuen, P., Spaak, J., Cars, O., Tängdén, T. & Lagerbäck, P. (2016) A novel microfluidic assay for rapid phenotypic antibiotic susceptibility testing of bacteria detected in clinical blood cultures. *Plos One*, **11**(12), e0167356.
 18. Gwaram, N. S., Ali, H. M., Khaledi, H., Abdulla, M. A., Hadi, H. A., Lin, T. K., Ching, C. L. & Ooi, C. L. (2012) Antibacterial evaluation of some Schiff bases derived from 2-acetylpyridine and their metal complexes. *Molecules*, **17**(5), 5952–5971.
 19. Low, M. L., Paulus, G., Dorlet, P., Guillot, R., Rosli, R., Delsuc, N., Crouse, K. A. & Policar, C. (2015) Synthesis, characterization and biological activity of Cu(II), Zn(II) and Re(I) complexes derived from *S*-benzylidithiocarbazate and 3-acetylcoumarin. *BioMetals*, **28**(3), 553–566.
 20. Aesar, A. (2020) Safety Data Sheet [3-methoxybenzoyl chloride]. *ThermoFisher Scientific*.
 21. Tarafder, M. T. H., Khoo, T. J., Crouse, K. A., Ali, A. M., Yamin, B. M. & Fun, H. K. (2002) Coordination chemistry and bioactivity of some metal complexes containing two isomeric bidentate NS Schiff bases derived from *S*-benzylidithiocarbazate and the X-ray crystal structures of *S*-benzyl- β -*N*-(5-methyl-2-furylmethylene) dithiocarbazate and bis[*S*-benzyl- β -*N*-(2-furylmethylketone) dithiocarbazate] cadmium (II). *Polyhedron*, **21**(27–28), 2691–2698.
 22. Pavia, D. L., Lampman, G. M., Kriz, G. S. & Vyvyan, J. R. (2015) *Introduction to spectroscopy*, Cengage Learning, USA.
 23. Ali, I., Wani, W. A. & Saleem, K. (2013) Empirical formulae to molecular structures of metal complexes by molar conductance. *Synthesis and Reactivity in Inorganic, Metal-Organic and Nano-Metal Chemistry*, **43**(9), 1162–1170.
 24. Wahba, M., El-Tabl, A. S., Abd-El Wahed, M. M., Wahba, M. A., EL-assaly, S. A. & Saad, L. M. (2015) Sugar hydrazone complexes; synthesis, spectroscopic characterization and antitumor activity. *Journal of Advances in Chemistry*, **9**(1).
 25. Xuan Hung, N., Anh Quang, D., Thanh Tam Toan, T., -, al, Guk, A., Krasnovskaya, O. O., Beloglazkina, E. K., Mahmoud, W. A., M. Hassan, Z. & Russel W. Ali (2020) Synthesis and spectral analysis of some metal complexes with mixed Schiff base ligands 1-[2-(2-hydroxybenzylidene-amino)ethyl]pyrrolidine-2,5-dione (HL1) and (2-hydroxybenzalidine)glycine (HL2). *Journal of Physics: Conference Series*, **1660**(1), 012027.
 26. Abdalrazaq, E. A., Al-Ramadane, O. M. & Al-Numa, K. S. (2010) Synthesis and characterization of dinuclear metal complexes stabilized by tetradentate Schiff base ligands. *American Journal of Applied Sciences*, **7**(5), 628–633.

27. Emam, S. M., El-Saied, F. A., Abou El-Enein, S. A. & El-Shater, H. A. (2009) Cobalt (II), nickel (II), copper (II), zinc (II) and hafnium (IV) complexes of N'-(furan-3-ylmethylene)-2-(4-methoxyphenylamino)acetohydrazide. *Spectrochimica Acta Part A: Molecular and Biomolecular Spectroscopy*, **72(2)**, 291–297.
28. Lever, A. B. P. (1984) Inorganic electronic spectroscopy. *Studies in Physical and Theoretical Chemistry*, **33**, 863.
29. Guo, L., Wu, S., Zeng, F. & Zhao, J. (2006) Synthesis and fluorescence property of terbium complex with novel Schiff-base macromolecular ligand. *European Polymer Journal*, **42(7)**, 1670–1675.
30. Chen, Z., Wu, Y., Gu, D. & Gan, F. (2007) Spectroscopic, and thermal studies of some new binuclear transition metal(II) complexes with hydrazone ligands containing acetoacetanilide and isoxazole. *Spectrochimica Acta Part A: Molecular and Biomolecular Spectroscopy*, **68(3)**, 918–926.
31. Ramesh, P., Adil, H. A., Mohammeda, N. -S., Siddappa, S., Muralidhar Reddy, P. & Pasha, C. (2016) Copper(II) complexes of new carboxamide ligands: synthesis, spectroscopic and antibacterial study. *International Journal of Advanced Research in Chemical Science (IJARCS)*, **3(8)**, 1–8.
32. El-Samanody, E. S. A., AbouEl-Enein, S. A. & Emara, E. M. (2018) Molecular modelling, spectral investigation and thermal studies of the new asymmetric Schiff base ligand; (E)-N'-(1-(4-((E)-2-hydroxybenzylideneamino)phenyl) ethylidene) morpholine-4-carbothiohydrazide and its metal complexes: Evaluation of their antibacterial and anti-molluscicidal activity. *Applied Organometallic Chemistry*, **32(4)**, e4262.
33. Bhat, R. A. (2019) Synthesis characterisation and theoretical studies of some transition metal complexes of dithiocarbazate Schiff bases and their potential biological activity investigations. *Thesis, Jiwaji University*.
34. Costa, A. R., de Menezes, T. I., Nascimento, R. R., dos Anjos, P. N. M., Viana, R. B., de Araujo Fernandes, A. G. & Santos, R. L. S. R. (2019) Ruthenium(II) dimethylsulfoxide complex with pyrazole/dithiocarbazate ligand: Synthesis, spectroscopy studies, DFT calculations and thermal behavior. *Journal of Thermal Analysis and Calorimetry*, **138(2)**, 1683–1696.
35. Raman, N., Muthuraj, V., Ravichandran, S. & Kulandaisamy, A. (2003) Synthesis, characterisation and electrochemical behaviour of Cu(II), Co(II), Ni(II) and Zn(II) complexes derived from acetylacetone and p-anisidine and their antimicrobial activity. *Journal of Chemical Sciences* **2003**, **115(3)**, 161–167.
36. Lobana, T. S., Sharma, R., Bawa, G. & Khanna, S. (2009) Bonding and structure trends of thiosemicarbazone derivatives of metals—An overview. *Coordination Chemistry Reviews*, **253(7–8)**, 977–1055.
37. Bhattacharjee, A., Das, S., Das, B. & Roy, P. (2021) Intercalative DNA binding, protein binding, antibacterial activities and cytotoxicity studies of a mononuclear copper(II) complex. *Inorganica Chimica Acta*, **514**, 119961.
38. Kargar, H., Aghaei-Meybodi, F., Behjatmanesh-Ardakani, R., Elahifard, M. R., Torabi, V., Fallah-Mehrjardi, M., Tahir, M. N., Ashfaq, M. & Munawar, K. S. (2021) Synthesis, crystal structure, theoretical calculation, spectroscopic and antibacterial activity studies of copper (II) complexes bearing bidentate Schiff base ligands derived from 4-amino-anti-pyridine: Influence of substitutions on antibacterial activity. *Journal of Molecular Structure*, **1230**, 129908.
39. Angelucci, F., Sayed, A. A., Williams, D. L., Boumis, G., Brunori, M., Dimastrogiovanni, D., Miele, A. E., Pauly, F. & Bellelli, A. (2009) Inhibition of schistosoma mansoni thioredoxin-glutathione reductase by Auranofin. Structural and kinetic aspects. *Journal of Biological Chemistry*, **284(42)**, 28977–28985.
40. Harbut, M. B., Vilchèze, C., Luo, X., Hensler, M. E., Guo, H., Yang, B., Chatterjee, A. K., Nizet, V., Jacobs, W. R., Schultz, P. G. & Wang, F. (2015) Auranofin exerts broad-spectrum bactericidal activities by targeting thiol-redox homeostasis. *Proceedings of the National Academy of Sciences of the United States of America*, **112(14)**, 4453–4458.
41. Sheikhshoaie, I., Ebrahimipour, S. Y., Lotfi, N., Mague, J. T. & Khaleghi, M. (2016) Synthesis, spectral characterization, X-ray crystal structure and antimicrobial activities of two cis dioxido-vanadium(V) complexes incorporating unsymmetrical dimalonitrile-based (NNO) Schiff base ligands. *Inorganica Chimica Acta*, **442**, 151–157.